

BIFURCATIONS OF SELF-SIMILAR SOLUTIONS FOR REVERSING INTERFACES IN THE SLOW DIFFUSION EQUATION WITH STRONG ABSORPTION

J. M. FOSTER*, P. GYSBERS†, J. R. KING‡, AND D. E. PELINOVSKY§

Abstract. Bifurcations of self-similar solutions for reversing interfaces are studied in the slow diffusion equation with strong absorption. The self-similar solutions bifurcate from the time-independent solutions for standing interfaces. We show that such bifurcations occur at the bifurcation points, at which the confluent hypergeometric functions satisfying Kummer’s differential equation is truncated into a finite polynomial. A two-scale asymptotic method is employed to obtain the asymptotic dependencies of the self-similar reversing interfaces near the bifurcation points. The asymptotic results are shown to be in excellent agreement with numerical computations.

Keywords: slow diffusion equation, strong absorption, self-similar solutions, reversing interface, bifurcations, Kummer’s differential equation, matched asymptotic expansions.

1. Introduction. We address reversing interfaces in the following slow diffusion equation with strong absorption

$$(1.1) \quad \frac{\partial h}{\partial t} = \frac{\partial}{\partial x} \left(h^m \frac{\partial h}{\partial x} \right) - h^n,$$

where $h(x, t)$ is a positive function on a compact support, *e.g.*, a concentration of some species, and x and t denote space and time, respectively. Restricting the exponents to the ranges $m > 0$ and $n < 1$ limits our interest to the case of slow diffusion [14] and strong absorption [15, 16, 17], respectively. The restriction $m > 0$ implies that the edges of the compact support propagate with a finite speed [8], whilst for $n < 1$ compactly supported solutions extinct in a finite time [4]. These two results suggest that, for certain choices of initial data which lead to an initial expansion of the compact support, reversing of interfaces can occur. Here, we use the term “reversing of interfaces” to describe a scenario in which an advancing interface gives way to a receding interface; the term “anti-reversing” of an interface describes the converse, *i.e.*, a receding interfaces giving way to an advancing one. Such scenarios have been examined in this range of exponents previously in [6, 7]. For the special case when $m + n = 2$ it has been shown, in [9], that solutions can exhibit reversing interfaces but cannot display a “waiting time” where an interface remains static for some finite time. The behaviour of solutions local to the extinction time has also been examined in the limiting case when $m + n = 1$ in [10, 11] and in the case $m > 1$ and $n < 1$ in [5].

The slow diffusion equation with strong absorption, (1.1), is relevant in a wide variety of different physical processes and can be used as a model for: (i) the slow spreading of a slender viscous film over a horizontal plate subject to the action of gravity and a constant evaporation rate [2] (when $m = 3$ and $n = 0$); (ii) the dispersion of a biological population subject to a constant death-rate [13] (when $m = 2$ and $n = 0$); (iii) nonlinear heat conduction along a rod with a constant rate of heat loss [14] (when $m = 4$ and $n = 0$), and; (iv) fluid flows in porous media with a drainage rate driven by gravity or background flows [3, 20] (when $m = 1$ and either $n = 1$ or $n = 0$).

After selecting the origin of the spatial and temporal coordinates such that the region of positive h lies in $x > 0$ and the reversing or anti-reversing event occurs at $t = 0$ (at which time the interface is located at $x = 0$), a plausible local behaviour of interfaces is provided by the self-similar solutions in the form suggested in [6],

$$(1.2) \quad h(x, t) = (\pm t)^{\frac{1}{1-n}} H_{\pm}(\xi), \quad \xi = x(\pm t)^{-\frac{m+1-n}{2(1-n)}}, \quad \pm t > 0,$$

*Department of Mathematics, University of Portsmouth, Portsmouth, UK, PO1 2UP (jamie.foster@port.ac.uk).

†Department of Physics & Astronomy, McMaster University, Hamilton ON, Canada, L8S 4K1.

‡School of Mathematical Sciences, Nottingham University, Nottingham, UK, NG7 2RD.

§Department of Mathematics & Statistics, McMaster University, Hamilton ON, Canada, L8S 4K1.

where the functions H_{\pm} satisfy the following second-order ordinary differential equations (ODEs):

$$(1.3) \quad \frac{d}{d\xi} \left(H_-^m \frac{dH_-}{d\xi} \right) - \frac{m+1-n}{2(1-n)} \xi \frac{dH_-}{d\xi} = H_-^n - \frac{1}{1-n} H_-$$

and

$$(1.4) \quad \frac{d}{d\xi} \left(H_+^m \frac{dH_+}{d\xi} \right) + \frac{m+1-n}{2(1-n)} \xi \frac{dH_+}{d\xi} = H_+^n + \frac{1}{1-n} H_+.$$

The mass preserving free-boundary conditions for (1.1) are

$$(1.5) \quad h \rightarrow 0^+, \quad \frac{ds_{\pm}}{dt} = h^m \frac{\partial h}{\partial x} + h^n \left(\frac{\partial h}{\partial x} \right)^{-1} \quad \text{as } x \rightarrow s_{\pm}(t)^+,$$

where $x = s_{\pm}(t)$ is the location of the free boundary for positive and negative time respectively. The form of the self-similar solution (1.2) implies that the interface after and before a reversing or anti-reversing event is located at the positions given by

$$(1.6) \quad s_{\pm}(t) = \hat{\xi}_{\pm} (\pm t)^{\frac{m+1-n}{2(1-n)}},$$

where $\hat{\xi}_{\pm}$ are both constants with $\hat{\xi}_+$ being relevant for $t > 0$ whilst $\hat{\xi}_-$ is relevant for $t < 0$. Owing to (1.6), in addition to requiring $m > 0$ and $n < 1$, we are also restricted to $m+n > 1$ so that $s_{\pm}(t)$ has a physically reasonable behaviour in time with $\lim_{t \rightarrow \pm 0} \dot{s}_{\pm}(t) = 0$. For technical reasons described below (3.5), we also restrict the range of n to $-1 \leq n < 1$.

The conditions (1.5) and (1.6) imply that solutions to (1.3) and (1.4) are required to satisfy

$$(1.7) \quad H_{\pm} \rightarrow 0^+, \quad H_{\pm}^m \frac{dH_{\pm}}{d\xi} \rightarrow 0^+ \quad \text{as } \xi \rightarrow \hat{\xi}_{\pm}^+.$$

For reasons that will become clear shortly the far-field condition

$$(1.8) \quad H_{\pm} \sim \left(\frac{\xi}{A} \right)^{\frac{2}{m+1-n}} \quad \text{as } \xi \rightarrow +\infty$$

completes the specification of the relevant boundary value problems for the system (1.3)–(1.4). The constant $A > 0$ is determined from solving equation (1.3) and the same A is prescribed while solving equation (1.4). Requiring identical far-field behaviours in the solution of both (1.3) and (1.4) is tantamount to ensuring continuity of h across $t = 0$ with

$$(1.9) \quad \lim_{t \rightarrow 0} h(x, t) = \left(\frac{x}{A} \right)^{\frac{2}{m+1-n}}.$$

Existence of suitable solutions to the boundary-value problem (1.3), (1.4), (1.7), and (1.8) was first suggested in [6]. Later, this was elaborated in [7] with an analytic shooting method that made use of invariant manifold theory for dynamical systems in appropriately rescaled variables near the small and large values of H_{\pm} .

We note the existence of an exact solution to (1.3)–(1.4) in the form

$$(1.10) \quad H_{\pm}(\xi) = \left(\frac{(m+1-n)^2}{2(m+n+1)} \xi^2 \right)^{\frac{1}{m+1-n}}.$$

The conditions (1.7) and (1.8) are satisfied with $\hat{\xi}_{\pm} = 0$ and $A = A_Q$, where

$$(1.11) \quad A_Q := \left(\frac{2(m+1+n)}{(m+1-n)^2} \right)^{1/2}.$$

It is straightforward to verify that in the original spatial and temporal variables given by (1.2) the exact solution (1.10) corresponds to a time-independent solution to the slow diffusion equation (1.1) given by

$$(1.12) \quad h(x) = \left(\frac{(m+1-n)^2}{2(m+1+n)} x^2 \right)^{\frac{1}{m+1-n}}.$$

Hence, the interface is static for the exact solution in (1.10) or (1.12). Although this solution does not constitute a reversing or anti-reversing interface solution, it does play a central role in the bifurcation analysis. Henceforth we refer to (1.10) as the *primary branch* of self-similar solutions to (1.3) and (1.4).

Given that there is a key difference between the boundary-value problems for H_- and H_+ , we shall provide local analysis of the asymptotic expansions as $\xi \rightarrow \hat{\xi}_{\pm}^{\pm}$. Two types of the leading-order balance may occur here. The first possibility is the usual balance for porous-medium equations, in which the absorption term, $-h^n$, is negligible, *i.e.*

$$(1.13) \quad \frac{d}{d\xi} \left(H_{\pm}^m \frac{dH_{\pm}}{d\xi} \right) \sim \mp \frac{m+1-n}{2(1-n)} \hat{\xi}_{\pm} \frac{dH_{\pm}}{d\xi}.$$

In view of the boundary conditions (1.7), the balance (1.13) is valid for $\pm \hat{\xi}_{\pm} < 0$ and yields the following local behaviour

$$(1.14) \quad H_{\pm} \sim \left(\mp \frac{m(m+1-n)\hat{\xi}_{\pm}}{2(1-n)} (\xi - \hat{\xi}_{\pm}) \right)^{1/m} \quad \text{as } \xi \rightarrow \hat{\xi}_{\pm}.$$

The second possibility arises when the diffusion term is negligible, *i.e.*

$$(1.15) \quad \pm \frac{m+1-n}{2(1-n)} \hat{\xi}_{\pm} \frac{dH_{\pm}}{d\xi} \sim H_{\pm}^n.$$

The balance (1.15) is valid for $\pm \hat{\xi}_{\pm} > 0$ and yields the following local behaviour

$$(1.16) \quad H_{\pm}(\xi) \sim \left[\pm \frac{2(1-n)^2}{(m+1-n)\hat{\xi}_{\pm}} (\xi - \hat{\xi}_{\pm}) \right]^{1/(1-n)} \quad \text{as } \xi \rightarrow \hat{\xi}_{\pm}.$$

The asymptotic behaviours (1.14) and (1.16) were proven rigorously in [7] by using rescaling and dynamical system methods.

Unlike (1.13), equation (1.15) is of first order and the second degree of freedom should be checked in the usual way by the Liouville-Green (JWKB) method, whereby linearisation about (1.15) implies a contribution

$$(1.17) \quad \exp \left(\frac{|\hat{\xi}_{\pm}|}{2} \left(\frac{(m+1-n)|\hat{\xi}_{\pm}|}{2(1-n)^2} \right)^{\frac{m}{1-n}} (\xi - \hat{\xi}_{\pm})^{-\frac{m+n-1}{1-n}} \right)$$

to the local expansion and is therefore inadmissible, *i.e.*, each of the balances (1.13) and (1.15) contain only one degree of freedom, namely $\hat{\xi}_{\pm}$.

As $\xi \rightarrow +\infty$ the behaviour (1.8) arises from the balance

$$(1.18) \quad \pm \frac{m+1-n}{2(1-n)} \xi \frac{dH_{\pm}}{d\xi} \sim \pm \frac{1}{1-n} H_{\pm}.$$

Equation (1.18) is again of first order and linearising about (1.8) to reinstate the second possible degree of freedom leads in this case to

$$(1.19) \quad \exp \left(\mp \left(\frac{m+1-n}{2(1-n)} A^{\frac{1}{m+1-n}} \right)^2 \xi^{\frac{2(1-n)}{m+1-n}} \right)$$

for H_{\pm} respectively. Therefore, the second solution is inadmissible for H_- (lower sign), leaving a single degree of freedom (namely A) as $\xi \rightarrow +\infty$, while it is admissible for H_+ (upper sign). Again, the behaviour (1.8) was justified in [7] by using rescaling and dynamical system methods.

In summary, ODEs (1.3) and (1.4) are to be solved subject to the boundary conditions (1.7) and hence (1.14) or (1.16) as $\xi \rightarrow \hat{\xi}_{\pm}^{\pm}$, where $\hat{\xi}_{\pm}^{\pm}$ is determined as a part of the solution H_{\pm} . In terms of the dynamics of the PDE (1.1), the local behaviour of the solutions switches from

$$(1.20) \quad h(x, t) \sim (-m\dot{s}(x-s))^{\frac{1}{m}} \quad \text{with } \dot{s} < 0,$$

as in (1.14), to

$$(1.21) \quad h(x, t) \sim \left(\frac{1-n}{\dot{s}}(x-s) \right)^{\frac{1}{1-n}} \quad \text{with } \dot{s} > 0,$$

as in (1.16) (or vice versa). The parameter A in the boundary condition (1.8) is determined as a part of the solution H_- by using a single-parameter shooting from either $\xi \rightarrow \hat{\xi}_{-}^{\pm}$ or $\xi \rightarrow +\infty$. The value of A is prescribed as a part of the solution H_+ .

A numerical shooting method was developed in [7] for the case $n = 0$ to connect the near-field and far-field behaviours for (1.3). The connection is possible only for some isolated values of A denoted by A^* . This shooting method was used here to obtain a diagram of some possible self-similar solutions in the (A, m) -plane for few selected values of n , see figure 1.1. For each point on these diagrams, there is a unique value of $\hat{\xi}_{-}$ which is positive on the red curves, negative on blue curves, and zero on black curves. A short summary of how the plots in figure 1.1 were produced is given in §5 and full details can be found in [7].

In addition to providing a scheme for connection of the relevant behaviours for the ODE (1.3) the work in [7] also demonstrated that all values of A in the behaviour (1.8) lead to a valid solution to the ODE (1.4) for H_+ . Moreover, it was shown that $\hat{\xi}_{+}$ is a monotonic increasing function of A with the following properties: if $A < A_Q$ then $\hat{\xi}_{+} < 0$, if $A > A_Q$ then $\hat{\xi}_{+} > 0$ whereas if $A = A_Q$ then $\hat{\xi}_{+} = 0$. Thus, if a valid solution to (1.3) can be found, a related solution to (1.4) can always be constructed for the same value of $A = A^*$.

The rather exotic patterns visible on figure 1.1 depict the existence of bifurcating solutions from the black curve that corresponds to the case $\hat{\xi}_{-} = 0$, and hence to the exact solution (1.10). In particular, we see that bifurcations appear to occur at

$$(1.22) \quad m = (2k-1)(1-n), \quad k \in \mathbb{N}.$$

It is natural to conjecture that there is a countable number of bifurcations as m increases beyond the values shown in the figure.

The present paper addresses bifurcations of self-similar solutions for reversing and anti-reversing interfaces from the exact solution (1.10). We refer to the bifurcating solutions as the *secondary branches*, which emerge from the primary branch. Since the existence of self-similar solutions is defined by the ODE (1.3), the rest of this work focusses on analysis of this equation only. Although our methods work for every $-1 \leq n < 1$, $m > 0$, and $m+n > 1$, we will simplify many details by considering the case $n = 0$ and $m > 1$ only.

The paper is organized as follows. §2 gives a quick review of properties of Kummer's differential equation. §3 reports the results on linearization of the ODE (1.3) at the exact solution (1.10). §4 describes a two-scale asymptotic method that allows us to obtain the secondary branches near the bifurcation points by superposing the bifurcating mode on the primary branch. In §5 we compare the predictions of the asymptotic method to numerical solutions and observe a good agreement between the two. Finally, §6 offers physical interpretations of new self-similar solutions obtained in this work.

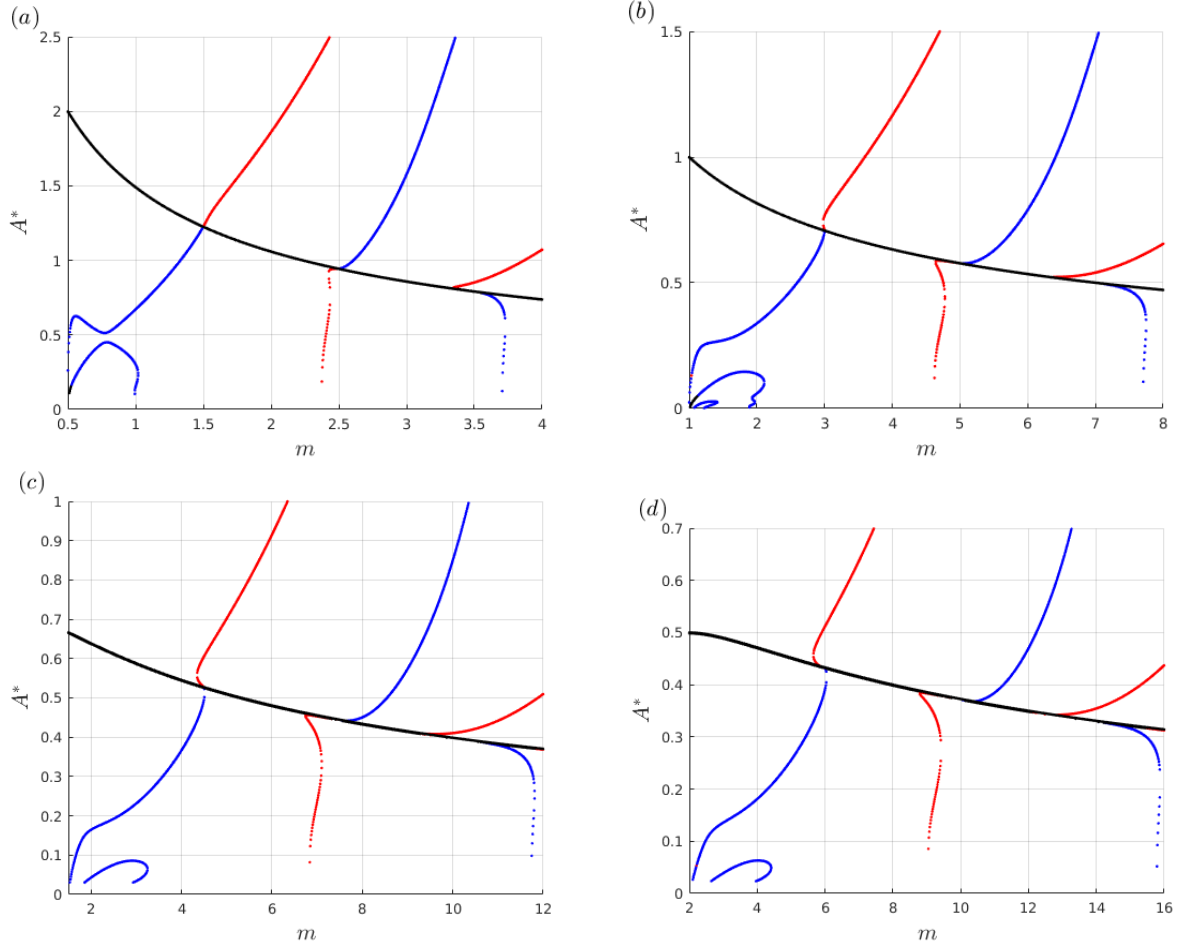


FIG. 1.1. The special values of $A = A^*$ (as a function of m) in the behaviour (1.8) that correspond to a solution of the ODE (1.3) with the near field behaviours (1.14) and (1.16). The red, blue and black curves indicates values of A^* that are associated with solutions with $\hat{\xi}_- > 0$, $\hat{\xi}_- < 0$, and $\hat{\xi}_- = 0$ respectively. Panels (a)-(d) show the results for values of $n = 1/2, 0, -1/2, -1$ respectively.

2. Kummer's differential equation. Kummer's differential equation for the confluent hypergeometric functions is defined as follows:

$$(2.1) \quad z \frac{d^2 w}{dz^2} + (b - z) \frac{dw}{dz} - aw = 0, \quad z \in \mathbb{R}^+,$$

where $a, b \in \mathbb{R}$ are parameters. We refer the reader to either Chapter 13 in [1] or Section 9.2 in [12] for a review of confluent hypergeometric functions.

The second-order ODE (2.1) has a regular singular point at $z = 0$ with two indices

$$\sigma_1 = 0, \quad \sigma_2 = 1 - b,$$

and in what follows we consider $b > 1$ when $\sigma_2 < \sigma_1$. If b is not a non-positive integer (which is the case for our setting), there exists a unique (up to a multiplicative constant) bounded solution at $z = 0$ given by the

following Kummer's function [18]

$$(2.2) \quad M(z; a, b) := \sum_{n \in \mathbb{N}_0} \frac{a_n z^n}{b_n n!} = 1 + \frac{a}{b} \frac{z}{1!} + \frac{a(a+1)}{b(b+1)} \frac{z^2}{2!} + \frac{a(a+1)(a+2)}{b(b+1)(b+2)} \frac{z^3}{3!} + \dots$$

where $a_0 = 1$, $a_1 = a$, and $a_n = a(a+1)\dots(a+n-1)$.

The other singular point of the second-order ODE (2.1) is $z = \infty$ and it is an irregular point with two linearly independent solutions

$$(2.3) \quad w_1(z) \sim z^{-a}, \quad w_2(z) \sim z^{a-b} e^z \quad \text{as } z \rightarrow \infty.$$

There exists a unique (up to a multiplicative constant) solution with the algebraic growth at infinity given by the following Tricomi function [22]

$$(2.4) \quad U(z; a, b) := \frac{\Gamma(1-b)}{\Gamma(1+a-b)} M(z; a, b) + \frac{\Gamma(b-1)}{\Gamma(a)} z^{1-b} M(z; 1+a-b, 2-b),$$

such that the function $U(z; a, b)$ satisfies the asymptotic expansion at infinity (see 13.1.8 in [1]):

$$(2.5) \quad U(z; a, b) = z^{-a} [1 + \mathcal{O}(|z|^{-1})] \quad \text{as } z \rightarrow +\infty.$$

If a is not a non-positive integer, then $U(z; a, b)$ is singular as $z \rightarrow 0$:

$$(2.6) \quad U(z; a, b) = \frac{\Gamma(b-1)}{\Gamma(a)} z^{1-b} [1 + \mathcal{O}(z)] \quad \text{as } z \rightarrow 0,$$

whereas $M(z; a, b)$ diverges at infinity (see 13.1.4 in [1]):

$$(2.7) \quad M(z; a, b) = \frac{\Gamma(b)}{\Gamma(a)} z^{a-b} e^z [1 + \mathcal{O}(|z|^{-1})] \quad \text{as } z \rightarrow +\infty.$$

If a is a non-positive integer, that is, if $a = -k$ with $k \in \mathbb{N}_0 := \{0, 1, 2, \dots\}$, then Kummer's function $M(z; a, b)$ is truncated into a polynomial of degree k so that $M(z; a, b)$ and $U(z; a, b)$ are linearly dependent. In §3, we reduce the linearized equation to Kummer's differential equation (2.1) and obtain the connection formulas between $M(z; a, b)$ and $U(z; a, b)$ for a non-positive integer a .

3. Linearization about the exact solution. The exact solution (1.10) with the definition (1.11) can be written as

$$(3.1) \quad H_Q(r) = r^{\frac{2}{m+1-n}},$$

where $r := \xi/A_Q$. The differential equation (1.3) is linearized at the exact solution (3.1) by writing $H_- = H_Q + u$ and truncating at the linear terms in u . By doing so, we obtain the homogeneous linear equation $Lu = 0$, where for $r \in \mathbb{R}^+$,

$$(3.2) \quad (Lu)(r) := \frac{(m+1-n)^2}{2(m+1+n)} \frac{d^2}{dr^2} \left(r^{\frac{2m}{m+1-n}} u(r) \right) - \frac{m+1-n}{2(1-n)} r \frac{du}{dr} + \frac{1}{1-n} u(r) - nr^{-\frac{2(1-n)}{m+1-n}} u(r).$$

It is necessary to equip the differential equation $Lu = 0$ with suitable boundary conditions at $r = 0$ and $r = \infty$. In order to consider the boundary conditions at $r = 0$, let us use the following transformation of the independent variable

$$(3.3) \quad y := \frac{m+1-n}{1-n} r^{\frac{1-n}{m+1-n}},$$

which allows us to rewrite the linear homogeneous equation $Lu = 0$ in the form

$$(3.4) \quad \frac{(m+1-n)^2}{2(m+1+n)} \left[\frac{d^2u}{dy^2} + \frac{3m}{(1-n)y} \frac{du}{dy} + \frac{2(m+n)(m-n-1)}{(1-n)^2y^2} u(y) \right] - \frac{1}{2} y \frac{du}{dy} + \frac{1}{1-n} u(y) = 0,$$

where we have used the same notation u as a function of $y \in \mathbb{R}^+$.

Use of the Frobenius method (see Chapter 4 in [21]) reveals that $y = 0$ is a regular singular point of the differential equation (3.4) with two indices $\sigma_{1,2}$ given by the indicial equation

$$(3.5) \quad \sigma(\sigma-1) + \frac{3m}{1-n}\sigma + \frac{2(m+n)(m-n-1)}{(1-n)^2} = 0 \quad \Rightarrow \quad \sigma_1 = \frac{1+n-m}{1-n}, \quad \sigma_2 = -\frac{2(n+m)}{1-n}.$$

We note that $\sigma_2 < \sigma_1$ for $m+3n+1 > 0$, which is satisfied if $m+n > 1$ and $1+n \geq 0$. Therefore, in what follows, we assume that $-1 \leq n < 1$. As follows from the Frobenius method and the indicial equation (3.5), there exist two linearly independent solutions of the differential equation (3.4) with the following behaviours near $y = 0$:

$$(3.6) \quad u_1(y) \sim y^{\frac{1+n-m}{1-n}} \quad \Rightarrow \quad u_1(r) \sim r^{\frac{1+n-m}{m+1-n}}$$

and

$$(3.7) \quad u_2(y) \sim y^{-\frac{2(n+m)}{1-n}} \quad \Rightarrow \quad u_2(r) \sim r^{-\frac{2(n+m)}{m+1-n}}.$$

In order to consider the boundary conditions at $r = \infty$ (or equivalently $y = \infty$), let us use the following transformation of the dependent variable

$$(3.8) \quad u(y) = y^{-\frac{3m}{2(1-n)}} \exp\left(\frac{m+1+n}{4(m+1-n)^2} y^2\right) v(y).$$

On using (3.8), the linear homogeneous equation (3.4) can be rewritten in the form

$$(3.9) \quad -\frac{d^2v}{dy^2} + \left[\frac{m^2 + 2m + 6mn + 8n^2 + 8n}{4(1-n)^2y^2} - \frac{(3m+5-n)(m+1+n)}{2(1-n)(m+1-n)^2} + \frac{(m+1+n)^2y^2}{4(m+1-n)^4} \right] v(y) = 0.$$

The linear equation (3.9) is well-known in quantum mechanics as the stationary Schrödinger equation for the multi-dimensional harmonic oscillator [19]. Owing to the harmonic confinement of the quantum oscillator, there is only one linear independent solution of the differential equation (3.9) that decays to zero as $y \rightarrow \infty$; the other solution grows rapidly as $y \rightarrow \infty$. Using the Liouville-Green (JWKB) method, it can be shown that the two linearly independent solutions behave at infinity as

$$(3.10) \quad v_1(y) \sim y^{\frac{3m+4}{2(1-n)}} \exp\left(-\frac{m+1+n}{4(m+1-n)^2} y^2\right) \Rightarrow u_1(r) \sim r^{\frac{2}{m+1-n}}$$

and

$$(3.11) \quad v_2(y) = y^{-\frac{3m+6-2n}{2(1-n)}} \exp\left(\frac{m+1+n}{4(m+1-n)^2} y^2\right) \Rightarrow u_2(r) \sim r^{-\frac{3(m+1)-n}{m+1-n}} \exp\left(\frac{m+1+n}{2(1-n)^2} r^{\frac{2(1-n)}{m+1-n}}\right).$$

The first solution matches the asymptotic behavior (1.8), whereas the second solution grows too fast and must be removed. Thus, in agreement with the invariant manifold result of Theorem 1.2 in [7], there is a unique (up to a normalizing constant) solution of the linear homogeneous equation $Lu = 0$, where L is given by (3.2), which satisfies suitable behaviour at infinity.

The stationary Schrödinger equation (3.9) for the multi-dimensional harmonic oscillator is solved in quantum mechanics at the admissible energy levels [19]. These energy levels correspond to the eigenfunctions v of

the linear equation (3.9), which belongs to $L^2(\mathbb{R}_+)$. For the function u satisfying the homogeneous equation $Lu = 0$, where L is given by (3.2), the admissible energy levels arise from the condition that the algebraically growing solution (3.10) at infinity is connected to the slowest algebraically growing solution (3.6) at zero.

Compared to this conventional treatment of the stationary Schrödinger equation (3.9), we will need to clarify the role of both algebraically growing solutions (3.6) and (3.7) at zero in the context of the self-similar solutions of the ODE (1.3). Therefore, we need a general solution of the stationary Schrödinger equation (3.9) satisfying (3.10), which is the only behaviour allowed there for the self-similar solutions of the ODE (1.3).

In order to reduce the stationary Schrödinger equation (3.9) to the Kummer differential equation (2.1), we transform both the dependent and independent variables as follows:

$$(3.12) \quad z := \frac{(m+1+n)}{2(m+1-n)}y^2, \quad v(y) := z^{\frac{m+2+2n}{4(1-n)}} \exp\left(-\frac{z}{2}\right)w(z).$$

On doing so, the linear homogeneous equation (3.9) can be rewritten in the form

$$(3.13) \quad z \frac{d^2w}{dz^2} + \left[\frac{m+3+n}{2(1-n)} - z \right] \frac{dw}{dz} + \frac{m+1-n}{2(1-n)}w(z) = 0,$$

which coincides with Kummer's equation (2.1) for

$$(3.14) \quad a := -\frac{m+1-n}{2(1-n)}, \quad b := \frac{m+3+n}{2(1-n)}.$$

Kummer's function $M(z; a, b)$ defined by (2.2) behaves near zero like the first slowest growing solution (3.6) after the transformations (3.3), (3.8), and (3.12) have been used. If a is not a non-positive integer, then $M(z; a, b)$ satisfies (2.7), which corresponds to the second, fastest growing, solution (3.11) at infinity. If a is a non-positive integer, then $M(z; a, b)$ is truncated into a polynomial, which corresponds to the first, slowest growing, solution (3.10). This happens for $a = a_k$ and $b = b_k$, where

$$(3.15) \quad a_k := -k, \quad b_k := k + \frac{1+n}{1-n}, \quad k \in \mathbb{N}_0 := \{0, 1, 2, \dots\},$$

in which case,

$$(3.16) \quad m = m_k := (2k-1)(1-n), \quad k \in \mathbb{N}_0.$$

Note that the bifurcation points given by (3.16) coincide with (1.22), except for the additional point $m_0 = n-1$. Since we are only interested in values of $m > 0$ and $n < 1$ the bifurcation point at $m_0 = n-1 < 0$ can be ignored.

Let us state explicitly the polynomials arising at the first four bifurcation points:

$$(3.17) \quad k = 1 : M(z; a_1, b_1) = 1 - \frac{1-n}{2}z,$$

$$(3.18) \quad k = 2 : M(z; a_2, b_2) = 1 - \frac{2(1-n)}{3-n}z + \frac{(1-n)^2}{2(3-n)(2-n)}z^2,$$

$$k = 3 : M(z; a_3, b_3) = 1 - \frac{3(1-n)}{2(2-n)}z + \frac{3(1-n)^2}{2(2-n)(5-3n)}z^2$$

$$(3.19) \quad - \frac{(1-n)^3}{4(2-n)(5-3n)(3-2n)}z^3,$$

$$k = 4 : M(z; a_4, b_4) = 1 - \frac{4(1-n)}{5-3n}z + \frac{13(1-n)^2}{(5-3n)(3-2n)}z^2$$

$$(3.20) \quad - \frac{2(1-n)^3}{(5-3n)(3-2n)(7-5n)}z^3 + \frac{(1-n)^4}{4(5-3n)(3-2n)(7-5n)(4-3n)}z^4.$$

For every a and b , Tricomi's function $U(z; a, b)$ defined by (2.4) is the only solution of the Kummer's differential equation (2.1) satisfying the asymptotic behaviour (2.5), which corresponds to the slowest growing solution (3.10) at infinity, after the transformations (3.3), (3.8), and (3.12) have been used. If a is not a non-positive integer, then $U(z; a, b)$ satisfies (2.6), which corresponds to the fastest growing solution (3.7) near zero.

The projection of $U(z; a, b)$ to the fastest growing solution (3.7) near zero is defined by taking the limit for $b > 1$ (which is satisfied in our case for $m + 3n + 1 > 0$):

$$(3.21) \quad \begin{aligned} B(m) &:= \lim_{z \rightarrow 0} z^{b-1} U(z; a, b) = \frac{\Gamma(b-1)}{\Gamma(a)} = \frac{\Gamma\left(\frac{m+1+3n}{2(1-n)}\right)}{\Gamma\left(-\frac{m+1-n}{2(1-n)}\right)} \\ &= \pi^{-1} \Gamma\left(\frac{m+1+3n}{2(1-n)}\right) \Gamma\left(\frac{m+3-3n}{2(1-n)}\right) \sin\left(\frac{\pi(m+3-3n)}{2(1-n)}\right), \end{aligned}$$

where we have used the following continuation property of the Gamma function (see 8.334 in [12])

$$(3.22) \quad \Gamma(x)\Gamma(1-x) = \frac{\pi}{\sin \pi x}.$$

We note that $B(m_k) = 0$ at the bifurcation point (3.16) and

$$(3.23) \quad B'(m_k) = \frac{1}{2(1-n)} (-1)^{k+1} \Gamma\left(k + \frac{2n}{1-n}\right) \Gamma(k+1).$$

It is more difficult to compute the projection of $U(z; a, b)$ to the slowest growing solution (3.6) near zero at the bifurcation point $m = m_k$. The first term in (2.4) gives the projection to the slowest growing solution (3.6) which is characterized by the quantity

$$(3.24) \quad C(m_k) := \lim_{m \rightarrow m_k} \frac{\Gamma\left(-\frac{m+1+3n}{2(1-n)}\right)}{\Gamma\left(-\frac{m+1+n}{1-n}\right)} = \lim_{m \rightarrow m_k} \frac{\Gamma\left(\frac{m+2}{1-n}\right)}{\Gamma\left(\frac{m+3+n}{2(1-n)}\right)} \frac{\sin\left(\frac{\pi(m+2)}{1-n}\right)}{\sin\left(\frac{\pi(m+3+n)}{2(1-n)}\right)}.$$

Let us define

$$(3.25) \quad p := \frac{2n}{1-n}.$$

Then, the limit $m \rightarrow m_k$ in (3.24) yields the following explicit expression

$$(3.26) \quad C(m_k) = \begin{cases} (-1)^k \frac{\Gamma(2k+1+p)}{\Gamma(k+1+p)}, & p \notin \mathbb{Z} \\ 2(-1)^k \frac{(2k+p)!}{(k+p)!}, & p \in \mathbb{Z}, \quad k+p \in \mathbb{N}, \end{cases}$$

where the continuation formula (3.22) has been used as well as the elementary property $\Gamma(k+1) = k!$ for a positive integer k . The second term in (2.4) does not give a projection to the slowest growing solution (3.6) if $b_k - 1$ is not an integer, that is, when $p \notin \mathbb{Z}$. On the other hand, when $p \in \mathbb{Z}$, we have

$$(3.27) \quad z^{1-b_k} M(z; 1+a_k-b_k, 2-b_k) = z^{-k-p} M(z; -2k-p, 1-k-p)$$

and since $-2k-p < 1-k-p$, the function above is not defined if $1-k-p$ is a non-positive integer. In order to resolve the singularity, we note the limit 9.214 in [12] for $k+p \in \mathbb{N}$:

$$(3.28) \quad \lim_{b \rightarrow b_k} \frac{M(z; 1+a-b, 2-b)}{\Gamma(2-b)} = \begin{pmatrix} a-1 \\ k+p \end{pmatrix} z^{k+p} M(z; a, b_k).$$

Therefore, we obtain from (2.4) and (3.28) for $k + p \in \mathbb{N}$:

$$(3.29) \quad \begin{aligned} D(m_k) &:= \lim_{z \rightarrow 0} \lim_{m \rightarrow m_k} \frac{\Gamma(b-1)\Gamma(2-b)}{\Gamma(a)} z^{1-b} \frac{M(z; 1+a-b, 2-b)}{\Gamma(2-b)} \\ &= \binom{-1-k}{k+p} \lim_{m \rightarrow m_k} \frac{\Gamma(1-a) \sin \pi(1-a)}{\sin \pi(b-1)}, \end{aligned}$$

where the continuation formula (3.22) has been used. This yields

$$(3.30) \quad \begin{aligned} D(m_k) &= (-1)^{k+p} \frac{(2k+p)!}{k!(k+p)!} \lim_{m \rightarrow m_k} \frac{\Gamma\left(\frac{m-3(1-n)}{2(1-n)}\right) \sin\left(\pi\left(\frac{m-3(1-n)}{2(1-n)}\right)\right)}{\sin\left(\pi\left(\frac{m+3n+1}{2(1-n)}\right)\right)} \\ &= (-1)^{k+1} \frac{(2k+p)!}{(k+p)!}. \end{aligned}$$

Thus, for $p \in \mathbb{Z}$, we define

$$(3.31) \quad E(m_k) := C(m_k) + D(m_k) = (-1)^k \frac{(2k+p)!}{(k+p)!}.$$

Note that this expression is a limit of $C(m_k)$ in the first line of (3.26) when a non-integer p approaches an integer value.

In §4, the asymptotic formulas (3.15), (3.23), and (3.31) are incorporated into the construction of the self-similar solution to the ODE (1.3) near the bifurcation point $m = m_k$, $k \in \mathbb{N}$.

4. Two-scale asymptotic method for bifurcating solutions. Here we consider the differential equation (1.3) with $n = 0$, the latter simplification is made purely to reduce what would otherwise be cumbersome large equations. However, we do note that the cases $n \neq 0$ with $-1 \leq n < 1$ can be included in our asymptotic analysis. After the subscript is dropped, the second-order ODE (1.3) with $n = 0$ is written in the form:

$$(4.1) \quad \frac{d}{d\xi} \left(H^m \frac{dH}{d\xi} \right) - \frac{m+1}{2} \xi \frac{dH}{d\xi} = 1 - H.$$

We are looking for the monotonically increasing solution on $[\hat{\xi}, \infty)$ with

$$(4.2) \quad \begin{cases} H(\xi) \rightarrow 0, \\ H^m(\xi)H'(\xi) \rightarrow 0, \end{cases} \quad \text{as } \xi \rightarrow \hat{\xi}$$

and

$$(4.3) \quad H(\xi) \sim \left(\frac{\xi}{A} \right)^{\frac{2}{m+1}} \quad \text{as } \xi \rightarrow \infty,$$

for some $A > 0$, see (1.8), (1.14), and (1.16).

In §4.1, we consider suitable solutions near $\xi \gtrsim \hat{\xi}$ for small $\hat{\xi}$. In §4.2, we expand solutions near the exact solution

$$(4.4) \quad H_Q(\xi) = \left(\frac{\xi}{A_Q} \right)^{\frac{2}{m+1}}, \quad A_Q = \frac{\sqrt{2}}{\sqrt{m+1}},$$

which corresponds to the case $\hat{\xi} = 0$ for $n = 0$. Matching conditions between the two formal asymptotic expansions are considered in §4.3, where small $\hat{\xi}$ and $A - A_Q$ are uniquely defined in terms of $m - m_k$, where $m_k = (2k - 1)$, $k \in \mathbb{N}$ is the bifurcation point for $n = 0$. Particular computations for $k = 1, 2, 3, 4$ are given as examples of these bifurcations.

4.1. Inner scale. In order to study the behaviour of solutions both in the near field (near the interface at $\xi = \hat{\xi}$), and in the asymptotic limit $\hat{\xi} \rightarrow 0$ (that is, close to the bifurcation value $m = m_k$, $k \in \mathbb{N}$), we use the scaling transformation

$$(4.5) \quad \xi = \hat{\xi} + |\hat{\xi}|^{\frac{m+1}{m-1}} \eta, \quad H(\xi) = |\hat{\xi}|^{\frac{2}{m-1}} \mathcal{H}(\eta),$$

where \mathcal{H} satisfies the second-order ODE

$$(4.6) \quad \frac{d}{d\eta} \left(\mathcal{H}^m \frac{d\mathcal{H}}{d\eta} \right) = 1 + \frac{m+1}{2} \sigma \frac{d\mathcal{H}}{d\eta} + |\hat{\xi}|^{\frac{2}{m-1}} \left(\frac{m+1}{2} \eta \frac{d\mathcal{H}}{d\eta} - \mathcal{H} \right),$$

where $\sigma = \text{sign}(\hat{\xi})$. In the limit $\hat{\xi} \rightarrow 0$, the second-order ODE (4.6) is truncated to the autonomous equation, which can be integrated once with the boundary conditions obtained from (4.2):

$$(4.7) \quad \begin{cases} \mathcal{H}(\eta) \rightarrow 0, \\ \mathcal{H}^m(\eta) \mathcal{H}'(\eta) \rightarrow 0, \end{cases} \quad \text{as } \eta \rightarrow 0.$$

After truncation and integration, the resulting equation is

$$(4.8) \quad \mathcal{H}_0^m \frac{d\mathcal{H}_0}{d\eta} = \eta + \frac{m+1}{2} \sigma \mathcal{H}_0,$$

where \mathcal{H}_0 denotes the leading order of the solution \mathcal{H} after truncation. The first-order non-autonomous equation (4.8) is equivalent to the following planar dynamical system

$$(4.9) \quad \begin{cases} \dot{\eta} = \mathcal{H}_0^m, \\ \dot{\mathcal{H}}_0 = \eta + \frac{m+1}{2} \sigma \mathcal{H}_0, \end{cases}$$

where the dot denotes a derivative with respect to the ‘time’ variable τ . The point $(\eta, \mathcal{H}_0) = (0, 0)$ is the only equilibrium point of the planar system (4.9). If $m > 1$ (since $m + n > 1$ and $n = 0$), the equilibrium point $(0, 0)$ is located at the intersection of a center curve tangential to the straight line

$$(4.10) \quad E^c(0, 0) = \left\{ \eta = -\frac{m+1}{2} \sigma \mathcal{H}_0, \quad \mathcal{H}_0 \in \mathbb{R} \right\}$$

and an unstable (stable) curve for $\hat{\xi} > 0$ ($\hat{\xi} < 0$), which is tangential to the \mathcal{H}_0 -axis.

We are only interested in constructing a trajectory of the dynamical system (4.9) in the first quadrant where $\mathcal{H}_0 > 0$ and $\eta > 0$. If $\hat{\xi} > 0$ ($\sigma = +1$), the tangent line $E^c(0, 0)$ in (4.10) to the center curve is not located in the first quadrant. Therefore, there is a unique trajectory of the dynamical system (4.9) that departs from $(0, 0)$ in the first quadrant along the unstable curve and satisfies the exponential growth

$$\mathcal{H}_0(\tau) \sim h_0 \exp\left(\frac{m+1}{2} \tau\right), \quad \eta(\tau) \sim \frac{2h_0^m}{m(m+1)} \exp\left(\frac{m(m+1)}{2} \tau\right) \quad \text{as } \tau \rightarrow -\infty,$$

where $h_0 > 0$ is an arbitrary constant. This yields the asymptotic expression

$$(4.11) \quad \mathcal{H}_0(\eta) \sim \left(\frac{m(m+1)}{2} \eta \right)^{\frac{1}{m}} \quad \text{as } \eta \rightarrow 0,$$

which coincides with the asymptotic behaviour (1.14) for $n = 0$ in near-field after the change of variables (4.5).

If $\hat{\xi} < 0$ ($\sigma = -1$), the tangent line $E^c(0, 0)$ in (4.10) to the center curve is now located in the first quadrant. Since the other invariant curve is stable, there is a unique trajectory of the dynamical system (4.9) that departs from $(0, 0)$ in the first quadrant along the center curve. The trajectory satisfies

$$(4.12) \quad \mathcal{H}_0(\eta) \sim \frac{2}{m+1} \eta \quad \text{as } \eta \rightarrow 0,$$

which coincides with the asymptotic behaviour (1.16) for $n = 0$ in near-field after the change of variables (4.5).

If $\hat{\xi} > 0$ ($\sigma = +1$), it follows from the first-order equation (4.8) that if a solution originates from the point $(\eta, \mathcal{H}_0) = (0, 0)$ in the first quadrant, then \mathcal{H}_0 is an monotonically increasing function of η with no stopping points. If $\hat{\xi} < 0$ ($\sigma = -1$), the same can be concluded by a contradiction. Suppose there is a finite ‘time’ τ_0 and a finite $\mathcal{H}_0(\tau_0) > 0$ such that $\dot{\mathcal{H}}_0(\tau_0) = 0$. Then, it follows from the system (4.9) that $\dot{\mathcal{H}}_0(\tau_0) = \dot{\eta}(\tau_0) = \mathcal{H}_0^m(\tau_0) > 0$, so that τ_0 is a minimum of \mathcal{H}_0 as a function of τ_0 . However, this contradicts to the fact that \mathcal{H}_0 was an increasing function of τ for $\tau < \tau_0$.

Thus, for both $\hat{\xi} > 0$ and $\hat{\xi} < 0$, the unique solution of the first-order equation (4.8) reaches infinity and since the right-hand side of the second equation in system (4.9) is linear in \mathcal{H}_0 , the solution cannot reach infinity in a finite η . Therefore, the unique solution satisfies $\mathcal{H}_0 \rightarrow \infty$ as $\eta \rightarrow \infty$. In order to derive the asymptotic behavior of the solution near infinity, we rewrite (4.8) following another integration with respect to η . We have

$$(4.13) \quad \frac{1}{m+1} \mathcal{H}_0^{m+1} = \frac{1}{2} \eta^2 + \frac{m+1}{2} \sigma \int_0^\eta \mathcal{H}_0(\eta') d\eta'.$$

It is now easy to obtain the asymptotic behaviour of \mathcal{H}_0 as $\eta \rightarrow \infty$ by iteration. We find that

$$(4.14) \quad \mathcal{H}_0(\eta) \sim \left(\frac{m+1}{2} \eta^2 \right)^{\frac{1}{m+1}} \quad \text{as } \eta \rightarrow \infty.$$

This behaviour coincides with the asymptotic behaviour (4.3) with $A = A_Q$ and $n = 0$ in the far-field after the change of variables (4.5).

Summarizing, we have proved the existence of a unique solution to the truncated first-order equation (4.8) which satisfies the leading-order asymptotic expansions (4.11) or (4.12) at zero and the leading-order asymptotic expansion (4.14) at infinity. The behaviour at infinity for the full solution $\mathcal{H}(\eta)$ is subject to the remainder terms proportional to $|\hat{\xi}|^{2/(m-1)}$ in the second-order equation (4.6).

We note that the expansion near infinity with the leading-order term in (4.14) is only understood in the asymptotic sense. It was proved in [7] that the trajectory of the differential equation (4.1) that originates at $H(\hat{\xi}) = 0$ and extends to $H(\xi) > 0$ for $\xi > \hat{\xi}$ does not generally reach infinity but turns back towards smaller values of H . It is only for special values of $\hat{\xi}$, that this trajectory reaches infinity to give curves on the solution diagram of Figure 1.1. In order to find these special values of $\hat{\xi}$, in the limit of small $\hat{\xi}$, *i.e.*, near the bifurcations, we need to construct the outer expansion and to deduce the asymptotic matching conditions on the two-scale expansions.

4.2. Outer scale. Let us consider solutions of the ODE (4.1) in the neighborhood of the exact solution (4.4), which is defined for every $\xi > 0$. To do so, we use the following regular asymptotic expansion:

$$(4.15) \quad H(\xi) = H_Q(r) + \alpha u_1(r) + \alpha^2 u_2(r) + \mathcal{O}(\alpha^3), \quad r := \frac{\xi}{A_Q},$$

where $\alpha \in \mathbb{R}$ is the small parameter in the formal expansion and the correction terms $\{u_1, u_2, \dots\}$ are to be defined recursively subject to appropriate boundary conditions.

Inserting the expansion (4.15) into (4.1) and balancing terms at $\mathcal{O}(\alpha)$, we obtain the homogeneous linear equation $Lu_1 = 0$, where the linear operator L is given by (3.2) with $n = 0$. We have proved in §3 that there is only one solution of the homogeneous equation $Lu_1 = 0$ (up to a multiplicative factor given by α), which satisfies the slowest growing behaviour (3.10) as $r \rightarrow \infty$. This solution is given by Tricomi’s function $U(z; a, b)$ in (2.4). After employing the transformations (3.3), (3.8), (3.12), and (3.14) with $n = 0$, we can define u_1 in terms of r as

$$(4.16) \quad u_1(r) = r^{\frac{1-m}{1+m}} U \left(\frac{m+1}{2} r^{\frac{2}{m+1}}; -\frac{m+1}{2}, \frac{m+3}{2} \right).$$

Proceeding to balance terms at $\mathcal{O}(\alpha^2)$, we obtain the linear inhomogeneous equation

$$(4.17) \quad Lu_2 = R_2 := -\frac{m(m+1)}{4} \frac{d^2}{dr^2} \left[r^{\frac{2(m-1)}{m+1}} u_1^2 \right].$$

Owing to the asymptotic behaviour (3.10) for $u_1(r)$ as $r \rightarrow \infty$, $R_2(r)$ is bounded as $r \rightarrow \infty$ and converges to a constant. Similarly, we observe that

$$Lr^{\frac{2}{m+1}} = (m+1),$$

therefore, there exists a solution of the inhomogeneous equation (4.17) satisfying the same asymptotic behaviour (3.10) at infinity. This solution is defined up to the choice of the homogeneous solution proportional to u_1 given by (4.16). Altering this choice of the homogeneous solution simply corresponds to redefining the small parameter α in the expansion (4.15). Therefore, without loss of generality, the homogeneous solution can be removed from the definition of $u_2(r)$, which then becomes uniquely defined.

Now, let us consider the behavior of solutions of the inhomogeneous equation (4.17) near $r = 0$. From (3.21) with $n = 0$, we know that

$$(4.18) \quad U(z; a, b) \sim B(m)z^{-\frac{m+1}{2}} \quad \text{as } z \rightarrow 0.$$

From (4.16), this yields the asymptotic behaviour

$$(4.19) \quad u_1(r) \sim B(m)2^{\frac{m+1}{2}}(m+1)^{-\frac{m+1}{2}}r^{-\frac{2m}{m+1}} \quad \text{as } r \rightarrow 0.$$

If $B(m) \neq 0$, then $R_2(r) \sim r^{-4}$ as $r \rightarrow 0$, so that the linear inhomogeneous equation (4.17) produces the solution (up to a multiplicative factor)

$$(4.20) \quad u_2(r) \sim B(m)r^{-\frac{4m+2}{m+1}}, \quad \text{as } r \rightarrow 0.$$

If $B(m) \neq 0$, the outer expansion (4.15) becomes singular with the fastest growth as $r \rightarrow 0$, which cannot be matched with the inner expansion obtained from (4.5) and (4.14). However, we show in §4.3 that the inner and outer expansions can be matched together near $m = m_k$ for some $k \in \mathbb{N}$ since $B(m_k) = 0$.

Recall that for $n = 0$, we have $p = 0$ in (3.25), so that both (3.26) and (3.30) are used to yield (3.31) for $m = m_k$, $k \in \mathbb{N}$. By using (4.16), we find

$$(4.21) \quad m = m_k : \quad u_1(r) = E(m_k)r^{\frac{1-m}{1+m}}M\left(\frac{m+1}{2}r^{\frac{2}{m+1}}; -k, k+1\right),$$

where $E(m_k)$ is defined by (3.31). By using (4.17), we obtain the inhomogeneous term of the linear equation in the following form,

$$(4.22) \quad R_2(r) = -\frac{m(m+1)}{4}E(m_k)^2\frac{d^2}{dr^2}\left[M^2\left(\frac{m+1}{2}r^{\frac{2}{m+1}}; -k, k+1\right)\right].$$

Since $M(z; -k, k+1)$ is a polynomial of degree k in z given by (2.2), the source term contains powers of $r^{2(-m+\ell)/(m+1)}$ for the integer ℓ counted from 0 to $m = m_k = 2k - 1$ with the missing factor at $\ell_k = (m-1)/2 = k-1$. The dominant term $r^{-2m/(m+1)}$ in $R_2(r)$ generates the same term in the solution $u_2(r)$ since

$$Lr^{-\frac{2m}{m+1}} = (m+1)r^{-\frac{2m}{m+1}}.$$

Therefore, in the case $B(m_k) = 0$, we obtain

$$(4.23) \quad u_2(r) \sim F(m_k)r^{-\frac{2m}{m+1}} \quad \text{as } r \rightarrow 0,$$

where $F(m_k)$ is computed from a linear algebraic system. Note that the dominant term in (4.23) is comparable with the dominant term (4.19) in the solution u_1 for $m \neq m_k$.

4.3. Matching conditions. Here we match the two (inner and outer) asymptotic regions together. Using the scaling transformation (4.5) and the leading-order behaviour (4.14), we obtain the dominant term of the inner expansion as follows

$$(4.24) \quad H(\xi) \sim \left(\frac{\xi - \hat{\xi}}{A_Q} \right)^{\frac{2}{m+1}}, \quad \text{as } \frac{\xi - \hat{\xi}}{|\hat{\xi}|^{\frac{m+1}{m-1}}} \rightarrow \infty \quad \text{and} \quad \hat{\xi} \rightarrow 0.$$

Expanding as $\hat{\xi} \rightarrow 0$ and using r as in (4.15), we obtain

$$(4.25) \quad H(\xi) \sim r^{\frac{2}{m+1}} - \frac{2\hat{\xi}}{(m+1)A_Q} r^{\frac{1-m}{1+m}} + \frac{(1-m)\hat{\xi}^2}{2(m+1)} r^{-\frac{2m}{m+1}}, \quad \text{as } \frac{\xi - \hat{\xi}}{|\hat{\xi}|^{\frac{m+1}{m-1}}} \rightarrow \infty \quad \text{and} \quad \hat{\xi} \rightarrow 0.$$

We can see that the first two correction terms in (4.25) occur also in the first two perturbation terms of the outer expansion (4.15) seen in (4.19), (4.21), and (4.23). This suggests that two constraints should arise from the matching process. The first constraint on the slowest growing term defines the parameter α in terms of $\hat{\xi}$:

$$(4.26) \quad -\frac{2\hat{\xi}}{(m+1)A_Q} = \alpha E(m_k) + \mathcal{O}(\alpha(m - m_k), \alpha^2).$$

The second constraint on the fastest growing term defines $m - m_k$ in terms of either α or $\hat{\xi}$:

$$(4.27) \quad \frac{(1-m)\hat{\xi}^2}{2(m+1)} = \alpha B'(m_k)(m - m_k) 2^{\frac{m+1}{2}} (m+1)^{-\frac{m+1}{2}} + \alpha^2 F(m_k) + \mathcal{O}(\alpha(m - m_k)^2, \alpha^2(m - m_k), \alpha^3).$$

After α is eliminated from the system (4.26) and (4.27), we obtain an asymptotic approximation of the solution curve in the $(\hat{\xi}, m)$ -plane.

On the other hand, in the limit $r \rightarrow \infty$, we compare the outer asymptotic expansion (4.15) with the asymptotic behaviour (4.3) at infinity, where A is a parameter. From (2.5) and (4.16), we obtain a constraint that defines the parameter α in terms of $A - A_Q$:

$$(4.28) \quad \left(\frac{A_Q}{A} \right)^{\frac{2}{m+1}} = 1 + \alpha(m+1)^{\frac{m+1}{2}} 2^{-\frac{m+1}{2}} + \mathcal{O}(\alpha^2).$$

Equation (4.28) yields the asymptotic approximation of the solution curve in the $(A, \hat{\xi})$ -plane in view of equation (4.26) or in the (A, m) -plane in view of the dependence of $\hat{\xi}$ versus m .

The sign-alternation of $E(m_k)$ over $k \in \mathbb{N}$ given by (3.31) yields by virtue of (4.26) and (4.28) the sign alternation of the dependence $(A - A_Q)$ versus $\hat{\xi}$ near the bifurcation point where $A = A_Q$ and $\hat{\xi} = 0$. This fact explains why the location of the red and blue curves bifurcating above and below the black curve on figure 1.1 alternates between the two adjacent bifurcation points.

In order to compare our analytical and numerical approaches, let us now compute the asymptotic dependencies near the first four bifurcation points explicitly.

4.3.1. Behaviour local to $m = 1$: At $m = 1$, there exists a one-parameter family of exact solutions to the differential equation (4.1) given by

$$(4.29) \quad H(\xi) = a(\xi - \hat{\xi}), \quad \hat{\xi} = \frac{a^2 - 1}{a}, \quad a \in \mathbb{R}.$$

We show that the matching conditions (4.26), (4.27), and (4.28) recover the exact solution (4.29). This implies that no new solution branches bifurcate near $m = 1$.

On setting $k = 1$ and $n = 0$ in (3.23) and (3.31), we obtain $B'(1) = 1/2$ and $E(1) = -2$. Since $A_Q = 1$, the matching conditions (4.26) and (4.28) tell us that

$$(4.30) \quad \hat{\xi} = 2\alpha + \mathcal{O}(\alpha^2), \quad \frac{1}{A} = 1 + \alpha + \mathcal{O}(\alpha^2).$$

From (3.17) with $n = 0$, (4.21), and (4.22), we obtain $u_1(r) = r - 2$ and $R_2(r) = -1$. Since $Lr^0 = 1$ if $m = 1$ and $n = 0$, there is a unique solution $u_2(r) = -1$ of the linear equation (4.17), from which we obtain $F(1) = 0$ from (4.23). The matching condition (4.27) yields

$$(4.31) \quad m - 1 = \mathcal{O}(\alpha^2).$$

Although the approximation (4.31) may imply that $m \neq 1$ for $\alpha \neq 0$ (or $\hat{\xi} \neq 0$), let us observe the correspondence between the asymptotic solution (4.15) with $\xi = r$, given explicitly by

$$(4.32) \quad H(\xi) = \xi + \alpha(\xi - 2) - \alpha^2 + \mathcal{O}(\alpha^3),$$

and the exact solution (4.29) with $a = 1 + \alpha$, which yields (4.32) with the $\mathcal{O}(\alpha^3)$ remainder term being equal to zero. From (4.3), (4.29), and (4.32), we obtain

$$\hat{\xi} = \alpha \frac{2 + \alpha}{1 + \alpha}, \quad A = \frac{1}{1 + \alpha},$$

which shows that the remainder terms in the second formula (4.30) and in (4.31) are identically zero.

4.3.2. Behaviour local to $m = 3$: On setting $k = 2$ and $n = 0$ in (3.23) and (3.31), we obtain $B'(3) = -1$ and $E(3) = 12$. Since $A_Q = 1/\sqrt{2}$, we obtain from (4.26) and (4.28):

$$\hat{\xi} = -12\sqrt{2}\alpha + \mathcal{O}(\alpha^2), \quad \frac{A_Q}{A} = 1 + 8\alpha + \mathcal{O}(\alpha^2),$$

that is,

$$(4.33) \quad \hat{\xi} = 3(A - A_Q) + \mathcal{O}((A - A_Q)^2).$$

In order to use (4.27), we need to compute the coefficient $F(3)$ in (4.23) from a linear algebraic system. From (3.18) with $n = 0$, (4.21), and (4.22), we obtain

$$u_1(r) = 12 \left[r^{-\frac{1}{2}} - \frac{4}{3} + \frac{1}{3}r^{\frac{1}{2}} \right]$$

and

$$R_2(r) = 12^2 \left[-2r^{-\frac{3}{2}} + 2r^{-\frac{1}{2}} - \frac{2}{3} \right].$$

From (3.2) with $m = 3$ and $n = 0$ we have:

$$Lr^{\frac{1}{2}} = 4, \quad Lr^0 = 1 + \frac{3}{2}r^{-\frac{1}{2}}, \quad Lr^{-\frac{1}{2}} = 2r^{-\frac{1}{2}}, \quad Lr^{-\frac{3}{2}} = 4r^{-\frac{3}{2}},$$

and we can find a unique solution of the linear equation (4.17) in the form

$$u_2(r) = 12^2 \left[-\frac{1}{2}r^{-\frac{3}{2}} + r^{-\frac{1}{2}} - \frac{1}{6}r^{\frac{1}{2}} \right],$$

from which $F(3) = -72$. The matching condition (4.27) yields

$$-\frac{1}{4}\hat{\xi}^2 = \frac{1}{4}\alpha(3-m) - 72\alpha^2 + \mathcal{O}(\alpha(3-m)^2, \alpha^2(3-m), \alpha^3).$$

Substituting $\hat{\xi} = -12\sqrt{2}\alpha + \mathcal{O}(\alpha^2)$, we obtain

$$(4.34) \quad 3 - m = \mathcal{O}(\hat{\xi}^2).$$

Although the approximation (4.34) is not definite due to the cancelation of the linear term in $\hat{\xi}$, we will show numerically in §5 that the dependence of $3 - m$ is indeed quadratic with respect to $\hat{\xi}$, see figure 5.1(a). The precise constant of this quadratic dependence can only be computed if the outer expansion (4.15) is expanded to next order $\mathcal{O}(\alpha^3)$, which is not computed here. We also see on figure 5.1(b) that the approximation (4.33) agrees well with the numerical results.

4.3.3. Behaviour local to $m = 5$: On setting $k = 3$ and $n = 0$ in (3.23) and (3.31), we obtain $B'(5) = 6$ and $E(5) = -120$. Since $A_Q = 1/\sqrt{3}$, we obtain from (4.26) and (4.28):

$$\hat{\xi} = 120\sqrt{3}\alpha + \mathcal{O}(\alpha^2), \quad \frac{A_Q}{A} = 1 + 81\alpha + \mathcal{O}(\alpha^2),$$

that is,

$$(4.35) \quad \hat{\xi} = -\frac{40}{9}(A - A_Q) + \mathcal{O}((A - A_Q)^2).$$

The coefficient $F(5)$ in (4.23) is computed from a linear algebraic system. From (3.19) with $n = 0$, (4.21), and (4.22), we obtain

$$u_1(r) = -120 \left[r^{-\frac{2}{3}} - \frac{9}{4}r^{-\frac{1}{3}} + \frac{27}{20} - \frac{9}{40}r^{\frac{1}{3}} \right]$$

and

$$R_2(r) = 120^2 \left[-\frac{15}{2}r^{-\frac{5}{3}} + \frac{207}{16}r^{-\frac{4}{3}} - \frac{189}{20}r^{-\frac{2}{3}} + \frac{81}{16}r^{-\frac{1}{3}} - \frac{243}{320} \right].$$

Thanks to the algebra obtained from (3.2) for $m = 5$ and $n = 0$:

$$\begin{aligned} Lr^{\frac{1}{3}} &= 6, & Lr^0 &= 1 + \frac{10}{3}r^{-\frac{1}{3}}, & Lr^{-\frac{1}{3}} &= 2r^{-\frac{1}{3}} + \frac{4}{3}r^{-\frac{2}{3}}, \\ Lr^{-\frac{2}{3}} &= 3r^{-\frac{2}{3}}, & Lr^{-\frac{4}{3}} &= 5r^{-\frac{4}{3}} - \frac{2}{3}r^{-\frac{5}{3}}, & Lr^{-\frac{5}{3}} &= 6r^{-\frac{5}{3}}, \end{aligned}$$

we can find a unique solution of the linear equation (4.17) in the form

$$u_2(r) = 120^2 \left[-\frac{77}{80}r^{-\frac{5}{3}} + \frac{207}{80}r^{-\frac{4}{3}} - \frac{387}{80}r^{-\frac{2}{3}} + \frac{243}{64}r^{-\frac{1}{3}} - \frac{243}{320} \right],$$

from which $F(5) = -13860$. The matching condition (4.27) yields

$$-\frac{1}{3}\hat{\xi}^2 = \frac{2}{9}\alpha(m-5) - 13860\alpha^2 + \mathcal{O}(\alpha(m-5)^2, \alpha^2(m-5), \alpha^3),$$

from which we obtain

$$(4.36) \quad 5 - m = \frac{27\sqrt{3}}{4}\hat{\xi} + \mathcal{O}(\hat{\xi}^2).$$

The asymptotic dependencies (4.35) and (4.36) will be compared with the numerical data in §5, where we will see the excellent agreement between them, see figure 5.2(a,b).

4.3.4. Behaviour local to $m = 7$. On setting $k = 4$ and $n = 0$ in (3.23) and (3.31), we obtain $B'(7) = -72$ and $E(7) = 1680$. Since $A_Q = 1/2$, we obtain from (4.26) and (4.28):

$$\hat{\xi} = -3360\alpha + \mathcal{O}(\alpha^2), \quad \frac{A_Q}{A} = 1 + 1024\alpha + \mathcal{O}(\alpha^2),$$

that is,

$$(4.37) \quad \hat{\xi} = \frac{105}{16}(A - A_Q) + \mathcal{O}((A - A_Q)^2).$$

The coefficient $F(7)$ in (4.23) is computed from a linear algebraic system. From (3.20) with $n = 0$, (4.21), and (4.22), we obtain

$$u_1(r) = 1680 \left[r^{-\frac{3}{4}} - \frac{16}{5}r^{-\frac{2}{4}} + \frac{16}{5}r^{-\frac{1}{4}} - \frac{128}{105} + \frac{16}{105}r^{\frac{1}{4}} \right]$$

and

$$R_2(r) = 1680^2 \left[-\frac{84}{5}r^{-\frac{7}{4}} + \frac{1456}{25}r^{-\frac{6}{4}} - \frac{1504}{25}r^{-\frac{5}{4}} + \frac{192}{5}r^{-\frac{3}{4}} - \frac{13568}{525}r^{-\frac{2}{4}} + \frac{512}{75}r^{-\frac{1}{4}} - \frac{1024}{1575} \right].$$

Thanks to the algebra obtained from (3.2) for $m = 7$ and $n = 0$:

$$\begin{aligned} Lr^{\frac{1}{4}} &= 8, & Lr^0 &= 1 + \frac{21}{4}r^{-\frac{1}{4}}, & Lr^{-\frac{1}{4}} &= 2r^{-\frac{1}{4}} + 3r^{-\frac{2}{4}}, & Lr^{-\frac{2}{4}} &= 3r^{-\frac{2}{4}} + \frac{5}{4}r^{-\frac{3}{4}}, \\ Lr^{-\frac{3}{4}} &= 4r^{-\frac{3}{4}}, & Lr^{-\frac{5}{4}} &= 6r^{-\frac{5}{4}} - r^{-\frac{6}{4}}, & Lr^{-\frac{6}{4}} &= 7r^{-\frac{6}{4}} - \frac{3}{4}r^{-\frac{7}{4}}, & Lr^{-\frac{7}{4}} &= 8r^{-\frac{7}{4}}, \end{aligned}$$

we can find a unique solution

$$u_2(r) = 1680^2 \left[-\frac{509}{350}r^{-\frac{7}{4}} + \frac{3616}{525}r^{-\frac{6}{4}} - \frac{752}{75}r^{-\frac{5}{4}} + \frac{4376}{315}r^{-\frac{3}{4}} - \frac{2898}{211}r^{-\frac{2}{4}} + \frac{128}{25}r^{-\frac{1}{4}} - \frac{1024}{1575} \right],$$

from which $F(7) = -4104576$. The matching condition (4.27) yields

$$-\frac{3}{8}\hat{\xi}^2 = \frac{9}{32}\alpha(7-m) - 4104576\alpha^2 + \mathcal{O}(\alpha(7-m)^2, \alpha^2(7-m), \alpha^3),$$

from which we obtain

$$(4.38) \quad 7 - m = \frac{2048}{15}\hat{\xi} + \mathcal{O}(\hat{\xi}^2).$$

The asymptotic dependencies (4.37) and (4.38) will be compared with the numerical data in §5, where we will see the excellent agreement between them, see figure 5.3(a,b).

5. Numerical results. Here we employ numerical methods to verify the analytical results obtained in §4.3. A fit scheme must be capable of furnishing numerical solutions to the ODE (1.3) which connect the far-field and near-field behaviours given by (1.8) and either (1.14) for $\hat{\xi}_- > 0$ or (1.16) for $\hat{\xi}_- < 0$. Such a numerical method has already been presented in [7] and so in the interests of brevity we will give a short summary — interested readers are referred to [7] for full details.

Finding numerical approximations of solutions for H_- is a problem that can be tackled using a shooting technique. An appropriate shooting parameter is the value of A in the far-field behaviour (1.8). On selecting a value for A the behaviour (1.8) can be used to define approximate initial data for $H_-(\xi)$ at some very large, yet finite, value of ξ to begin numerical integration of the ODE (1.3) in the direction of decreasing ξ . The

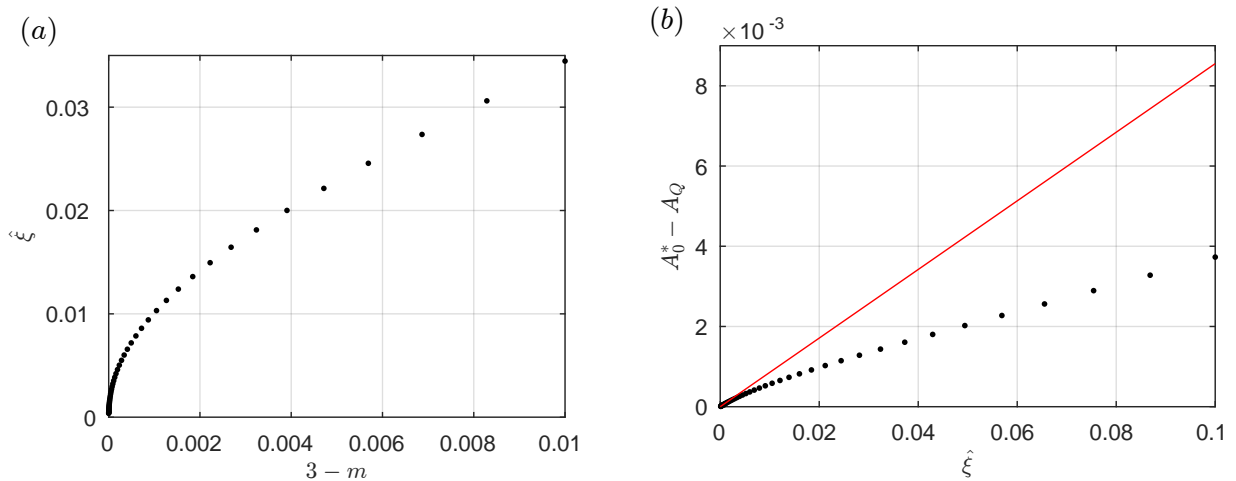


FIG. 5.1. Panel (a): The variation of $\hat{\xi}$ with $3 - m$ as predicted by shooting. The observed quadratic dependence of $3 - m$ on $\hat{\xi}$ is in agreement with (4.34). Panel (b): The variation of $A - A_Q$ with $\hat{\xi}$ local to $m = 3$ as predicted by both shooting (black dots) and (4.33) (red line).

integration can be continued until either the value of $H_-(\xi)$ or $H_-^m(\xi)H'_-(\xi)$ vanishes at some $\xi = \hat{\xi}$; it was proven in [7] that at least one of these two conditions will be reached for the unique solution satisfying (1.8). The solution to (1.3) we are looking for satisfy both of the aforementioned conditions. It is by iterating on the value of A that proper solution(s) for H_- can be found that satisfy both $H_-(\hat{\xi}_-) = 0$ and $H_-^m(\hat{\xi}_-)H'_-(\hat{\xi}_-) = 0$, for some $\hat{\xi}_-$. We denote the special value(s) of A that give rise to solutions satisfy these conditions by A^* .

Values of A^* as a function of m are shown in figure 1.1 when the exponent n of the absorption term in the slow diffusion equation (1.1) is set equal to $1/2, 0, -1/2, -1$. From these figures we observe that at each value of $m = m_k = (2k - 1)(1 - n)$ for $k \in \mathbb{N}$ two branches of solutions (one with $\hat{\xi}_- > 0$ (red) and the other with $\hat{\xi}_- < 0$ (blue)) bifurcate from the main black branch corresponding to the exact solution (1.10) with $\hat{\xi}_- = 0$. The bifurcation points were identified in §3, see (3.16). Moreover, the alternation of the red and blue curves above the black curve between adjacent bifurcations observed on figure 1.1 can be explained by the sign alternation of $E(m_k)$ in (3.31) and (4.26) between two values of k .

The matched asymptotics analysis in §4 yields prediction of the local dependencies of both $\hat{\xi}_-$ and $A^* - A_Q$ on $m_k - m$ local to each bifurcation point $m = m_k$ for $n = 0$. In figures 5.1-5.3 we show a comparison between these predictions and the results of the numerical shooting scheme outlined above. We observe excellent agreement in all cases, thereby supporting both the analysis presented here and the accuracy of the numerical scheme proposed in [7].

6. Conclusions. We conclude this paper by placing the self-similar solutions into the original physical context, *i.e.*, in terms of the PDE (1.1). On transforming to travelling wave-type coordinate system that moves with the position of the left-hand interface (with position $x = s(t)$), using the change of variables $\eta = x - s(t)$, and seeking asymptotic solutions to the PDE (1.1) for small values of the moving coordinate, η , we find solutions with local behavior in (1.20) for $\dot{s} < 0$ and in (1.21) for $\dot{s} > 0$. The local behaviour in (1.20) is termed an advancing interface, since its motion acts to enlarge the domain of compact support, whereas the local behaviour in (1.21) is termed a receding solution. Examining (1.20) we see that the advancing wave is largely controlled by the exponent m and the diffusive-type term in (1.1). Physically this corresponds to the forward motion of an interface being driven by fluid pressure ($m = 3$), a biological population pressure ($m = 2$) or nonlinear heat conduction ($m = 4$). Contrastingly, the alternative behaviour, (1.21), is controlled by the absorption term in (1.1) and relates the physical mechanisms of fluid evaporation or absorption into a substrate ($n = 0$ or $n = 1$), the constant death rate of a biological population ($n = 0$) or the loss of heat.

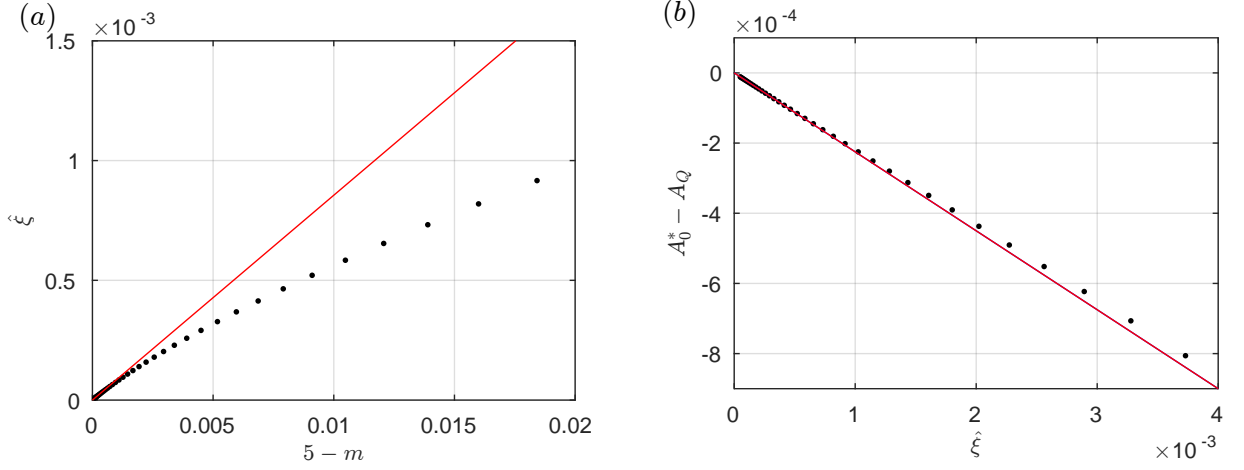


FIG. 5.2. Panel (a) shows the variation of $\hat{\xi}$ with $5 - m$ and panel (b) shows the variation of $A - A_Q$ with $\hat{\xi}$ local to $m = 5$. Black dots indicate numerical results whereas the red lines in panels (a) and (b) are the behaviours predicted by (4.35) and (4.36) respectively.

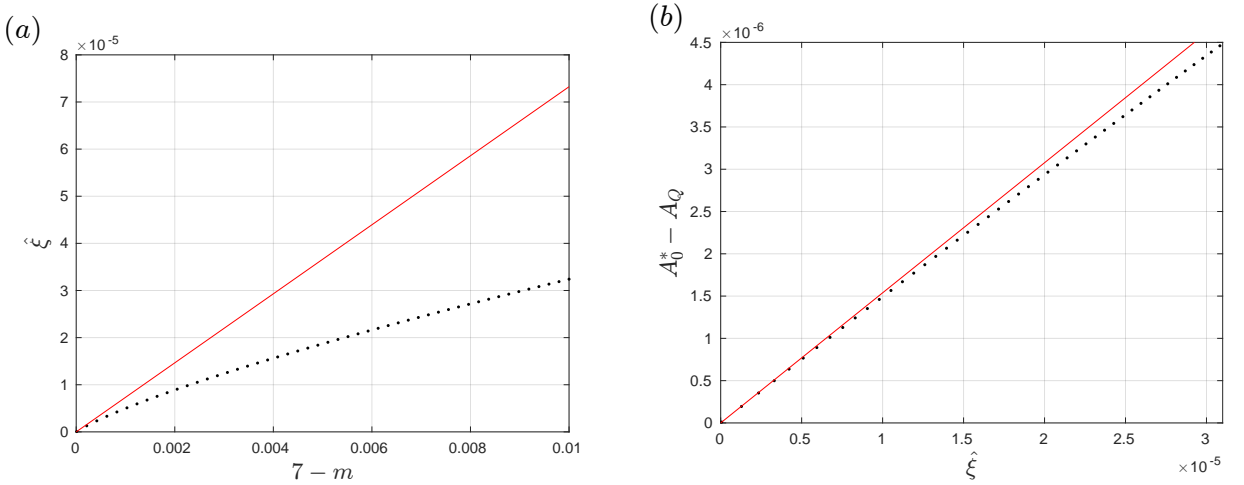


FIG. 5.3. Panel (a) shows the variation of $\hat{\xi}$ with $7 - m$ and panel (b) shows the variation of $A - A_Q$ with $\hat{\xi}$ local to $m = 7$. Black dots are numerical results whereas the red lines in panels (a) and (b) are the behaviours predicted by (4.37) and (4.38) respectively.

The physical motivation behind the current work is elucidating the processes by which the former local solution becomes the latter (a reversing solution) or vice versa (an anti-reversing solution). In addition to (anti-)reversing solutions we have also studied solutions which advance (recede) instantaneously halt/pause at $t = 0$ and then continue advancing (receding) corresponding to the former (latter) behaviour for both negative and positive t . Reversing solutions are manifested in the self-similar context by solutions for H_{\pm} with $\hat{\xi}_{\pm} > 0$. On referring to figure 1.1 we see that at least one such solution exist for all $m \gtrsim m_2$. Contrastingly, it seems that anti-reversing solutions, corresponding to $\hat{\xi}_{\pm} < 0$, exist for $m_1 < m < m_2$. The receding pausing ($\hat{\xi}_- > 0$ and $\hat{\xi}_+ < 0$) solutions emerge from the primary (black) branch at $m = m_3$ and persist for $m > m_3$. A branch of advancing pausing solutions ($\hat{\xi}_- > 0$ and $\hat{\xi}_+ < 0$) also emerge from the main branch at this point but persist only for a much smaller range of m .

Acknowledgements. J.F. was supported by a postdoctoral fellowship at McMaster University. He thanks B. Protas for hospitality and many useful discussions. The work of P.G. was performed within an undergraduate research project in physics at McMaster University. The authors are also grateful to A. D. Fitt for inspiration and useful discussions.

REFERENCES

- [1] HANDBOOK OF MATHEMATICAL FUNCTIONS WITH FORMULAS, GRAPHS, AND MATHEMATICAL TABLES, Eds. M. Abramowitz and I.A. Stegun (Dover Publications, NY, 1972).
- [2] J. M. ACTON, H.E. HUPPERT, AND M.G. WORSTER, *Two dimensional viscous gravity currents flowing over a deep porous medium*, J. Fluid Mech. 440 (2001), 359–380.
- [3] D. G. ARONSON, *Regularity properties of flows through porous media*, SIAM J. Appl. Math. 17 (1969), 461–467.
- [4] X. Y. CHEN, H. MATANO AND M. MIMURA, *Finite-point extinction and continuity of interfaces in a nonlinear diffusion equation with strong absorption*, J. reine angew. Math. 459 (1995), 1–36.
- [5] A. DE PABLO & J. L. VAZQUEZ, *The Balance Between Strong Reaction And Slow Diffusion*, Communications in Partial Differential Equations, 15 (1990), 159–183.
- [6] J. M. FOSTER, C. P. PLEASE, A. D. FITT, AND G. RICHARDSON, *The reversing of interfaces in slow diffusion processes with strong absorption*, SIAM J. Appl. Math. 72 (2012), 144–162.
- [7] J.M. FOSTER AND D.E. PELINOVSKY, *Self-similar solutions for reversing interfaces in the slow diffusion equation with strong absorption*, SIAM J. Appl. Dynam. Syst. 15 (2016), 2017–2050.
- [8] V. A. GALAKTIONOV, S. I. SHMAREV AND J. L. VAZQUEZ, *Regularity of interfaces in diffusion processes under the influence of strong absorption*, Arch. Rational Mech. Anal. 149 (1999), 183–212.
- [9] V. A. GALAKTIONOV, S. I. SHMAREV AND J. L. VAZQUEZ, *Behaviour of interfaces in a diffusion-absorption equations with critical exponents* Interfaces and Free Boundaries 2 (2000), 425–448.
- [10] V.A. GALAKTIONOV & J. L. VAZQUEZ, *Extinction for a quasilinear heat equation with absorption i. technique of intersection comparison*, Communications in Partial Differential Equations 19 (1994), 1075–1106.
- [11] V.A. GALAKTIONOV & J. L. VAZQUEZ, *Extinction for a quasilinear heat equation with absorption ii. a dynamical systems approach*, Communications in Partial Differential Equations 19 (1994), 1107–1137.
- [12] I.S. GRADSHTEYN AND I.M. RYZHIK, *Table of integrals, series and products*, 6th edition, Academic Press, San Diego, CA (2005)
- [13] M. E. GURTIN, *On the diffusion of biological populations*, Math. Biosci. 33 (1977), 35–49.
- [14] M.A. HERRERO AND J.L. VAZQUEZ, *The one-dimensional nonlinear heat equation with absorption: regularity of solutions and interfaces*, SIAM J. Math. Anal. 18 (1987), 149–167.
- [15] A. S. KALASHNIKOV, *The propagation of disturbances in problems of nonlinear heat conduction with absorption*, USSR Comput. Math. Phys. 14 (1974), 70–85.
- [16] B. KAWOHL AND R. KERSNER, *On degenerate diffusion with very strong absorption*, Math. Methods Appl. Sci. 15 (1992), 469–477.
- [17] R. KERSNER, *Nonlinear heat conduction with absorption: Space localization and extinction in finite time*, SIAM J. Appl. Math. 43 (1983), 1274–1285.
- [18] E.E. KUMMER, “De integralibus quibusdam definitis et seriebus infinitis”, Journal für die reine und angewandte Mathematik (in Latin) **17** (1837), 228–242.
- [19] L.D. LANDAU AND E.M. LIFSCHITZ *Quantum Mechanics* (Pergamon Press, Oxford, 1965).
- [20] D. PRITCHARD, A. W. WOODS AND A. J. HOGG, *On the slow draining of a gravity current moving through a layered permeable medium*, J. Fluid Mech. 444 (2001), 23–47.
- [21] G. TESCHL, *Ordinary Differential Equations and Dynamical Systems* (AMS, Providence, 2012).
- [22] F.G. TRICOMI, “Sulle funzioni ipergeometriche confluenti”, Annali di Matematica Pura ed Applicata, Serie Quarta (in Italian) **26** (1947), 141–175.